



Cite this: *Green Chem.*, 2021, **23**, 5456

Received 12th May 2021,  
Accepted 26th June 2021

DOI: 10.1039/d1gc01677f

rsc.li/greenchem

## Quasi-homogeneous catalytic conversion of CO<sub>2</sub> into quinazolinones inside a metal–organic framework microreactor†

Zhenzhen Zhou,<sup>a</sup> Jian-Gong Ma, \*<sup>a</sup> Jianbo Gao<sup>b</sup> and Peng Cheng \*<sup>a,c</sup>

Management of CO<sub>2</sub> has been attracting great attention in this century. Reaction of CO<sub>2</sub> with 2-haloanilines and isocyanides is an attractive way for both converting CO<sub>2</sub> and producing quinazolinones, which are key intermediates for the synthesis of various biologically active products. However, the heterogeneous and relatively inert nature of CO<sub>2</sub> with 2-haloaniline and isocyanide reactants limits the types of suitable catalysts. Herein, we use metal–organic frameworks (MOFs) as a “microreactor”, in which Pd(PPh<sub>3</sub>)<sub>2</sub>Cl<sub>2</sub> is well-dispersed as a single-molecular catalyst, and the reactants react in the molecular level through a “quasi-homogeneous” way to convert CO<sub>2</sub> into quinazolinones under mild conditions with both promising yields over homogeneous catalysts and good recyclability as a heterogeneous reaction. The MOF-assisted single-molecular catalysis strategy should contribute to CO<sub>2</sub> conversion, production of quinazolinone-type bioactive intermediates, and the epochal development of “homo-and-heterogeneous” catalysis.

Carbon dioxide has been attracting great attention in this century both as a major greenhouse gas and as an abundant, economical, nontoxic and renewable C<sub>1</sub> source.<sup>1</sup> Consequently, conversion of CO<sub>2</sub> into value-added chemical materials is of dual significance. Recently, reaction of CO<sub>2</sub> with 2-haloanilines and isocyanides exhibited a promising way both for fixation of CO<sub>2</sub> and for green production of quinazolinones,<sup>2</sup> which are key intermediates for the synthesis of a series of biologically active products and medicines.<sup>3</sup> However, because the reactants including CO<sub>2</sub> (gas), 2-haloanilines (solid) and isocyanides (liquid) are mutually heterogeneous, suitable catalysts

for such synthetic processes are extremely limited, and no heterogeneous catalyst has been reported yet.

Metal–organic frameworks (MOFs), composed of organic linkers with metal ions or clusters,<sup>4–6</sup> have exhibited wide potential applications in the management of CO<sub>2</sub> in recent years for their super adsorption capacity towards CO<sub>2</sub> due to their porous structure and ultrahigh surface area.<sup>7–25</sup> Herein, we make use of MOFs’ well-defined pores as a “microreactor” to provide an individual confined environment. For the first time, the organometallic Pd(PPh<sub>3</sub>)<sub>2</sub>Cl<sub>2</sub> is loaded and well-dispersed as a “single-molecular catalyst” in the pores of the MOF MIL-101(Cr), and the reactants 2-haloanilines and isocyanides are transported into the MOF pores by a solvent in the form of molecules, and CO<sub>2</sub> molecules are efficiently adsorbed into the pores by the MOF. As a result, the MOF acts as a “microreactor”, in which the reactants are arranged and react at the molecular level catalyzed by the single-molecular Pd(PPh<sub>3</sub>)<sub>2</sub>Cl<sub>2</sub> (**s-Pd(PPh<sub>3</sub>)<sub>2</sub>Cl<sub>2</sub>**) through a “quasi-homogeneous” way. This MOF reactor-based single-molecular approach enables the conversion of CO<sub>2</sub> into quinazolinones under 1 atm at a low temperature (50 °C), which exhibits promising activity and efficiency over homogeneous catalysts as well as good reusability like heterogeneous catalysts.

Pd(PPh<sub>3</sub>)<sub>2</sub>Cl<sub>2</sub> was selected as the active center for the reaction of CO<sub>2</sub> with 2-haloanilines and isocyanides, because of its specific activity towards C–X bond activation, C–C coupling and C–N bond formation as well as the moderate coordination ability and adjustable size of its phosphine group.<sup>26</sup> MIL-101(Cr) was used as a MOF microreactor due to its high stability, highly porous structure and cage-type pores with a suitable size (2.2–2.7 nm cavity diameter with 0.7 and 1.0 nm windows),<sup>27</sup> which allowed the entry of the PPh<sub>3</sub> ligand (0.9 nm) yet restricted the escape of the formed complex (1.2 nm).<sup>28</sup> The Pd(PPh<sub>3</sub>)<sub>2</sub>Cl<sub>2</sub> molecule was *in situ* assembled inside MIL-101’s cage by the “ship in a bottle” method, as shown in Scheme 1.

Synchrotron powder X-ray diffraction (PXRD) shows that MIL-101(Cr) is preserved intact during the assembly of the Pd(PPh<sub>3</sub>)<sub>2</sub>Cl<sub>2</sub> molecule inside the MOF cage (Fig. 1a), which is

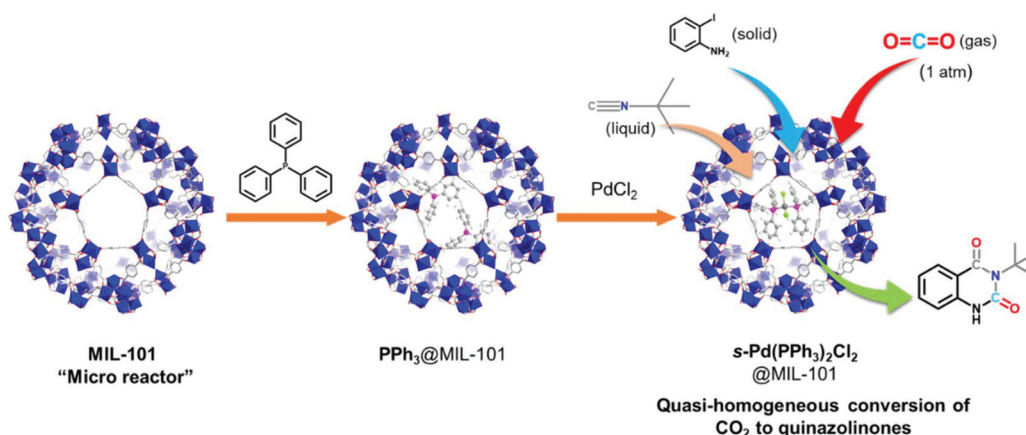
<sup>a</sup>Department of Chemistry, Key Laboratory of Advanced Energy Materials Chemistry (MOE) and Renewable Energy Conversion and Storage Center (RECAST), College of Chemistry, Nankai University, Tianjin 300071, P. R. China.

E-mail: mvbasten@nankai.edu.cn, pcheng@nankai.edu.cn

<sup>b</sup>Centre of Excellence for Advanced Materials, Dongguan 523808, P. R. China

<sup>c</sup>Frontiers Science Center for New Organic Matter, Nankai University, Tianjin 300071, P. R. China

† Electronic supplementary information (ESI) available. See DOI: 10.1039/d1gc01677f



**Scheme 1** Quasi-homogeneous conversion of CO<sub>2</sub> into quinazolinones over the single-molecularly dispersed catalyst in a MIL-101 microreactor.

further confirmed by the scanning electron microscopy (SEM) images (Fig. S1†). Solid-state NMR was used to confirm the presence and the coordination of PPh<sub>3</sub> with Pd ions. As shown in Fig. 1b, the solid-state NMR spectra of the encapsulated **s-Pd(PPh<sub>3</sub>)<sub>2</sub>Cl<sub>2</sub>** show exactly the same <sup>31</sup>P signals as those of the independent Pd(PPh<sub>3</sub>)<sub>2</sub>Cl<sub>2</sub>, indicating the successful loading of Pd(PPh<sub>3</sub>)<sub>2</sub>Cl<sub>2</sub> inside the pores of MIL-101(Cr), which is further confirmed by comparing the FT-IR spectra of Pd(PPh<sub>3</sub>)<sub>2</sub>Cl<sub>2</sub>, MIL-101(Cr), PPh<sub>3</sub>@MIL-101(Cr) and **s-Pd(PPh<sub>3</sub>)<sub>2</sub>Cl<sub>2</sub>@MIL-101**, as shown in Fig. 1d.<sup>23</sup> X-ray photoelectron spectroscopy (XPS) (Fig. 3) of **s-Pd(PPh<sub>3</sub>)<sub>2</sub>Cl<sub>2</sub>@MIL-101** shows a pattern quite similar to that of the Pd(PPh<sub>3</sub>)<sub>2</sub>Cl<sub>2</sub> compound, indicating the successful assembly of the Pd(PPh<sub>3</sub>)<sub>2</sub>Cl<sub>2</sub> molecules inside the MOF microreactor.<sup>29</sup> In the XPS spectra, the peaks at 335.2 eV and 340.4 eV are well-assigned to 3d<sub>5/2</sub> and 3d<sub>3/2</sub> of Pd(II), and no peak of Pd

(0) is observed, and the peak for Cl appears at 198.4 eV and 199.9 eV – the same as that in the Pd(PPh<sub>3</sub>)<sub>2</sub>Cl<sub>2</sub> compound, which unambiguously confirms the coordination environment of the Pd(II) center and the formation of Pd(PPh<sub>3</sub>)<sub>2</sub>Cl<sub>2</sub> molecules inside the MOF microreactor. Inductively Coupled Plasma (ICP) analysis shows the content of the Pd element loaded in MIL-101(Cr) as 4.65%. The incorporation of Pd(PPh<sub>3</sub>)<sub>2</sub>Cl<sub>2</sub> molecules is also illustrated by transmission electron microscopy (TEM) through the well dispersed Pd, P and Cl elements in elemental mapping and the Energy-Dispersive Spectroscopy (EDS) data (Fig. 2). The specific surface area, pore size and pore volume of MIL-101(Cr) after loading the Pd(PPh<sub>3</sub>)<sub>2</sub>Cl<sub>2</sub> molecules was measured by N<sub>2</sub> physisorption analysis at 77 K (Fig. 1c), exhibiting a typical completely reversible isotherm as the original MIL-101(Cr). The Brunauer–Emmett–Teller (BET) surface area (*S*<sub>BET</sub>) of MIL-101(Cr) and MIL-101

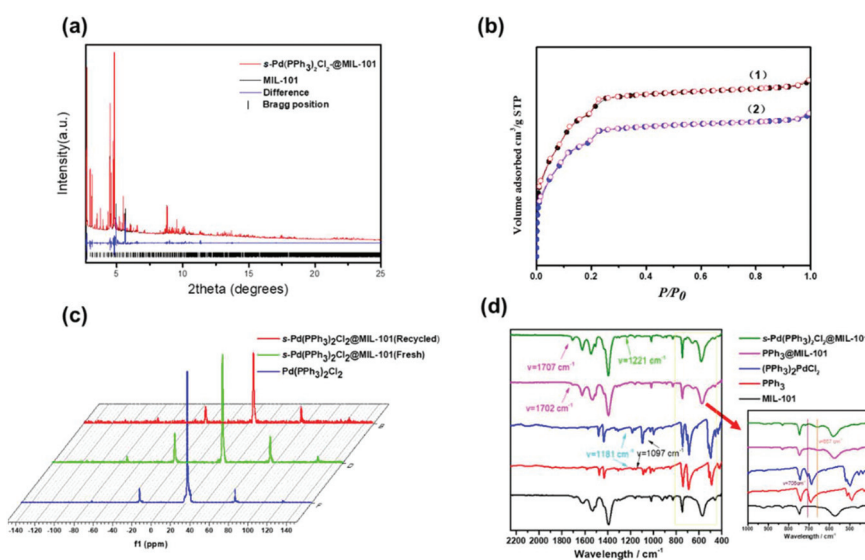


**Fig. 1** (a) Synchrotron PXRD of **s-Pd(PPh<sub>3</sub>)<sub>2</sub>Cl<sub>2</sub>@MIL-101**. (b) N<sub>2</sub> adsorption/desorption isotherms of (1) MIL-101(Cr) and (2) **s-Pd(PPh<sub>3</sub>)<sub>2</sub>Cl<sub>2</sub>@MIL-101** at 77 K. (c) Solid-state NMR of **s-Pd(PPh<sub>3</sub>)<sub>2</sub>Cl<sub>2</sub>@MIL-101**. (d) FT-IR spectra of MIL-101(Cr), PPh<sub>3</sub>, Pd(PPh<sub>3</sub>)<sub>2</sub>Cl<sub>2</sub>, PPh<sub>3</sub>@MIL-101 and **s-Pd(PPh<sub>3</sub>)<sub>2</sub>Cl<sub>2</sub>@MIL-101**.

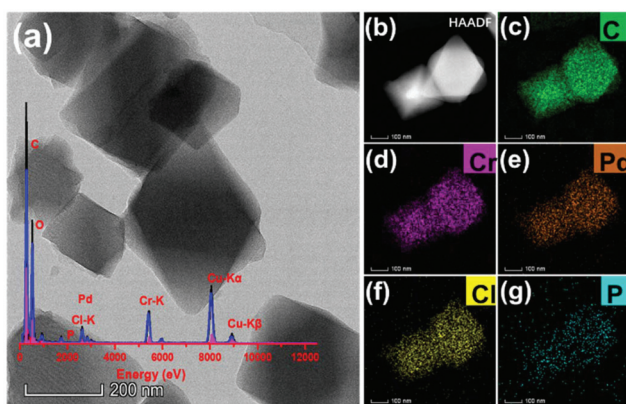


**Fig. 2** (a) TEM and EDS of *s*-Pd(PPh<sub>3</sub>)<sub>2</sub>Cl<sub>2</sub>@MIL-101. (b) HAADF-STEM images of (c) C, (d) Cr, (e) Pd, (f) Cl and (g) P.

(Cr) with Pd(PPh<sub>3</sub>)<sub>2</sub>Cl<sub>2</sub> are given as 2613 m<sup>2</sup> g<sup>-1</sup> and 1987 m<sup>2</sup> g<sup>-1</sup> with pore volumes (*V<sub>p</sub>*) 1.273 cm<sup>3</sup> g<sup>-1</sup> and 1.038 cm<sup>3</sup> g<sup>-1</sup>, respectively, demonstrating that the cavities of MIL-101(Cr) are occupied by the highly dispersed *s*-Pd(PPh<sub>3</sub>)<sub>2</sub>Cl<sub>2</sub>.

The MOF-loaded single-molecular catalyst *s*-Pd(PPh<sub>3</sub>)<sub>2</sub>Cl<sub>2</sub> was then applied to process the reaction of CO<sub>2</sub> with 2-haloanilines and isocyanides to produce quinazolinones. The reaction was carried out under ambient pressure in MeCN. As the temperature increased from 25 °C, the yield of the quinazolinone product increased from 62.2 to 91.9% at 50 °C in 18 h catalyzed by only 1 mol% *s*-Pd(PPh<sub>3</sub>)<sub>2</sub>Cl<sub>2</sub>, and then decreased when the temperature increased further (Table 1, entries 1–6). When 2 mol% catalyst was used, the yield decreased to 85.2% (Table 1, entry 6), probably because more catalyst blocked the MOF pores and affected the entrance of the reactant molecules and the exit of the product. 18 h was proven to be the optimized time for this reaction (Table 1, entries 8 and 9), and DBU and MeCN were confirmed as the optimized base and

solvent, respectively. After the reaction, we carried out hot filtration (Fig. S9†) and analyzed the Pd content of the filtrate by an ICP test, which suggested that the leaching of Pd is almost negligible (0.3 μg ml<sup>-1</sup>, *ca.* 0.02% of the catalyst).

With the optimized conditions in hand, we explored the substrate scope of various 2-iodoanilines **1a–i** (Table S2†). The reactions of 2-iodoanilines bearing the electron-donating groups such as methyl and methoxyl with isocyanide **2a** and CO<sub>2</sub> afforded the desired products **3c** and **3d** in more than 95% yields, and halogen-substituted 2-iodoanilines were used to produce **3e–i** in *ca.* 90% yields, which confirmed the broad application scope of *s*-Pd(PPh<sub>3</sub>)<sub>2</sub>Cl<sub>2</sub> with the MOF reactor.

To illustrate the outstanding activity of the single-molecular *s*-Pd(PPh<sub>3</sub>)<sub>2</sub>Cl<sub>2</sub> in the MOF reactor, we compared the activities of other known or relative catalysts under the optimized conditions. The results are summarized in Table 2. Without a catalyst, there is no product detected (Table 2, entry 2). When we used the MOF MIL-101 (Cr) alone, the reaction hardly took place (Table 2, entry 3), indicating the Pd complex as the catalytic active center. When using Pd(PPh<sub>3</sub>)<sub>2</sub>Cl<sub>2</sub> without the MOF reactor, the yield of the quinazolinone was only 41.5% (Table 2, entry 4), although Pd(PPh<sub>3</sub>)<sub>2</sub>Cl<sub>2</sub> is a homogeneous catalyst, which unambiguously confirms the significance of the MOF as a microreactor and the single-molecular dispersion of *s*-Pd(PPh<sub>3</sub>)<sub>2</sub>Cl<sub>2</sub>. The other relative Pd compounds including PdCl<sub>2</sub>, Pd(PPh<sub>3</sub>)<sub>4</sub> and Pd(OAc)<sub>2</sub> gave very poor yield of *ca.* 40%. The reported catalysts for this reaction were quite limited,<sup>2,3</sup> and they were homogeneous catalytic systems and required 10 times more Pd content, a higher temperature (80 °C) and even 10 bar (9.9 atm) CO<sub>2</sub> pressure.

From the industrial perspective, the recyclability of a catalyst is an important criterion for heterogeneous catalysis. The catalyst recycling experiment was performed on the same model reaction of introducing CO<sub>2</sub> into a multicomponent reaction of isocyanides. Upon completion of the reaction, the

**Table 1** Screening of the optimal reaction conditions<sup>a</sup>

Entry	Cat. (mol%)	Base	Solvent	Temp. (°C)	Yield (%)
1	1	DBU	MeCN	25	62.2
2	1	DBU	MeCN	40	60.3
3	1	DBU	MeCN	50	91.9
4	1	DBU	MeCN	60	89.4
5	1	DBU	MeCN	70	85.0
6	1	DBU	MeCN	80	90.5
7	2	DBU	MeCN	50	85.2
8 <sup>b</sup>	1	DBU	MeCN	50	85.4
9 <sup>c</sup>	1	DBU	MeCN	50	82.9

<sup>a</sup> Reaction conditions: **1a** (0.60 mmol), **2a** (0.90 mmol), catalyst *s*-Pd(PPh<sub>3</sub>)<sub>2</sub>Cl<sub>2</sub>@MIL-101 (1% mol based on Pd), base (0.1 equiv.), solvent (4 ml), Schlenk tube, CO<sub>2</sub> balloon, 50 °C, 18 h. <sup>b</sup> The reaction was carried out for 12 h. <sup>c</sup> The reaction was carried out for 10 h.

**Table 2** Screening of the compared reaction conditions<sup>a</sup>

Entry	Cat. (mol%)	Temp. (°C)	Yield (%)
1	<i>s</i> -Pd(PPh <sub>3</sub> ) <sub>2</sub> Cl <sub>2</sub> @MIL-101 (1)	50	91.9
2	—	50	0
3	MIL-101(Cr) (1)	50	Trace
4	Pd(PPh <sub>3</sub> ) <sub>2</sub> Cl <sub>2</sub> (1)	50	41.5
5	PdCl <sub>2</sub> (1)	50	44.9
6	Pd(PPh <sub>3</sub> ) <sub>4</sub> (1)	50	40.5
7	Pd(OAc) <sub>2</sub> (1)	50	39.5
8	Pd(PPh <sub>3</sub> ) <sub>2</sub> Cl <sub>2</sub> (1) + MIL-101(Cr) (1)	50	42
9	PdCl <sub>2</sub> (10) + PPh <sub>3</sub> (20)	80	92–97 (ref. 3)
10 <sup>b</sup>	Pd(OAc) <sub>2</sub> (10) + BuPAD <sub>2</sub> (20)	80	91 (ref. 2)

<sup>a</sup> Reaction conditions: **1a** (0.60 mmol), **2a** (0.90 mmol), catalyst, DBU base (0.1 equiv.), MeCN solvent (4 ml), Schlenk tube, CO<sub>2</sub> balloon, 18 h. <sup>b</sup> 10 bar CO<sub>2</sub>, Cs<sub>2</sub>CO<sub>3</sub> base, 1,4-dioxane solvent and 7–16 h.

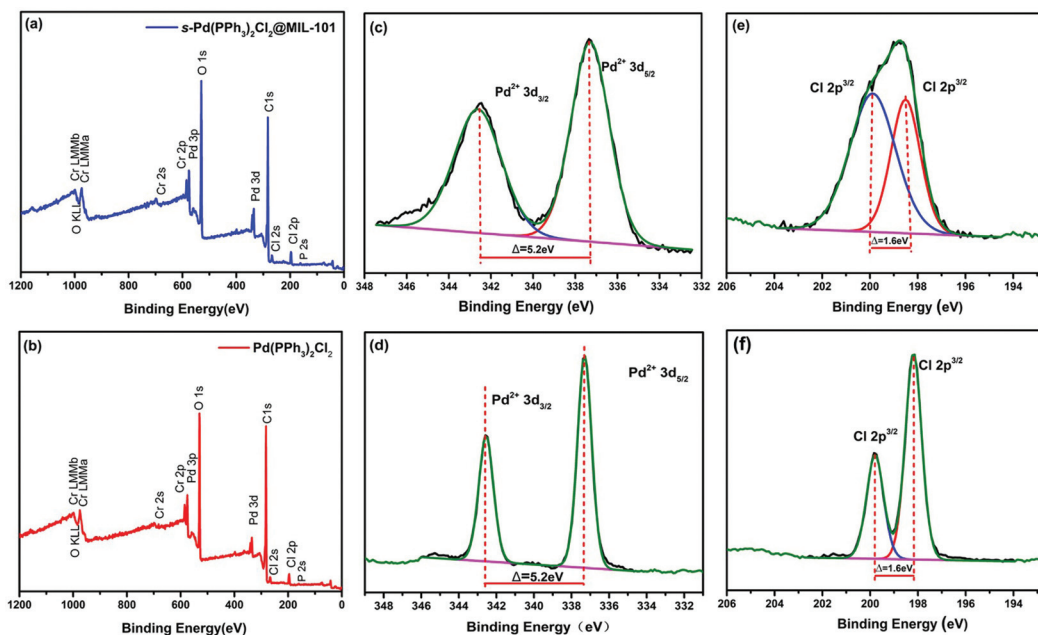


**Fig. 3** (a) The XPS full spectrum of *s*-Pd(PPh<sub>3</sub>)<sub>2</sub>Cl<sub>2</sub>@MIL-101. (b) The XPS full spectrum of pure Pd(PPh<sub>3</sub>)<sub>2</sub>Cl<sub>2</sub>. (c) After encapsulation of Pd spectrum. (d) Pd spectrum. (e) After encapsulation of Cl spectrum. (f) After encapsulation of Cl spectrum.

catalyst was separated from the reaction mixture by filtration, washed properly with dry ethanol and dried in a vacuum desiccator. The recycled catalyst was then used for the same reaction up to five consecutive cycles, which was fully characterized afterwards. ICP tests of the fresh and reused catalyst after five cycles confirmed the good recyclability of the composite catalyst (Table S1†) and suggested that the molar ratios of Pd : P for both the fresh and recycled catalyst matched the molecular formula of Pd(PPh<sub>3</sub>)<sub>2</sub>Cl<sub>2</sub> quite well, indicating the perfect reserve of the active center. The crystallinity of the support remained unaltered in the recovered catalyst, as shown in the TEM (Fig. S2†) images, and the dispersion of the Pd, P and Cl elements was well maintained, as shown in the EDS mapping (Fig. S3†) throughout the chemical transformation. According to the XPS analysis (Fig. S6†), the valence state of Pd in catalyst showed no change after five times experiment, and the solid-state NMR spectra of the recovered *s*-Pd(PPh<sub>3</sub>)<sub>2</sub>Cl<sub>2</sub>@MIL-101 showed exactly the same <sup>31</sup>P signals as those of the independent Pd(PPh<sub>3</sub>)<sub>2</sub>Cl<sub>2</sub> and fresh *s*-Pd(PPh<sub>3</sub>)<sub>2</sub>Cl<sub>2</sub>@MIL-101, which proved the maintenance of *s*-Pd(PPh<sub>3</sub>)<sub>2</sub>Cl<sub>2</sub> in the MOF cavity in the molecular form. The FT-IR spectra of the recovered catalyst (Fig. S5†) confirmed the intact structural properties of the recovered catalyst as well. Overall, all these characterization methods clearly show the heterogeneous nature of the MIL-101(Cr) supported single-molecular catalyst.

## Conclusions

In summary, we make use of the unique porous metal-organic frameworks (MOFs) as a “microreactor” to provide an individ-

ual environment. The catalyst Pd(PPh<sub>3</sub>)<sub>2</sub>Cl<sub>2</sub> is loaded and well-dispersed as a single molecule in the pores of the MOF MIL-101(Cr), and the reactants 2-haloanilines and isocyanides are transported into the MOF pores by a solvent in the form of molecules, and the CO<sub>2</sub> molecules are efficiently adsorbed into the pores by the MOF. It is the first time that phosphine compounds have been supported on MOFs as heterogeneous catalysts for chemical fixation of CO<sub>2</sub> to synthesize quinazolinones. This method is efficient and recyclable. MOFs are currently applied in more and more catalysis processes; thus, our molecular method may find vast use for efficiently enhancing the activities of MOF catalysts and remarkably saving the time and cost not only in CO<sub>2</sub> conversion but also in other synthetic procedures. Besides, the synthesis of new catalysts opens up a new direction for the synthesis of supported catalysts. It is of great significance for the catalytic application of MOFs.

## Conflicts of interest

There are no conflicts to declare.

## Acknowledgements

This work was supported by the National Key R&D Program of China (2016YFB0600902), the NSFC (21771112 and 21875120) and the Fundamental Research Funds for the Central Universities, Nankai University (63181206 and 63213060). Dr J. Gao acknowledged the support from the Program for Guangdong Introducing Innovative and Entrepreneurial Teams (2016ZT06G025). We acknowledge Dr Qinfen Gu of the

Australian Synchrotron (ANSTO) for performing synchrotron PXRD characterization.

## Notes and references

- S. Wang and C. Xi, *Chem. Soc. Rev.*, 2019, **48**, 382–404.
- P. Mampuy, H. Neumann, S. Sergeev, R. V. A. Orru, H. Jiao, A. Spannenberg, B. U. W. Maes and M. Beller, *ACS Catal.*, 2017, **7**, 5549–5556.
- P. Xu, F. Wang, T.-Q. Wei, L. Yin, S. Y. Wang and S. J. Ji, *Org. Lett.*, 2017, **19**, 4484–4487.
- A. Schneemann, V. Bon, I. Senkowska, S. Kaskel and R. A. Fischer, *Chem. Soc. Rev.*, 2014, **43**, 6062–6096.
- C.-J. Liu, N.-N. Zhu, J.-G. Ma and P. Cheng, *Research*, 2019, **2019**, 5178573.
- X.-Q. Wu, J.-G. Ma, H. Li, D.-M. Chen, W. Gu, G.-M. Yang and P. Cheng, *Chem. Commun.*, 2015, **51**, 9161–9164.
- M. H. Beyzavi, R. C. Klet, S. Tussupbayev, J. Borycz, N. A. Vermeulen, C. J. Cramer, J. F. Stoddart, J. T. Hupp and O. K. Farha, *J. Am. Chem. Soc.*, 2014, **136**, 15861–15864.
- W.-Y. Gao, Y. Chen, Y.-H. Niu, K. Williams, L. Cash, P. J. Perez, L. Wojtas, J.-F. Cai, Y.-S. Chen and S.-Q. Ma, *Angew. Chem., Int. Ed.*, 2014, **53**, 2615–2619.
- Y. E. Cheon and M. P. Sun, *Angew. Chem., Int. Ed.*, 2009, **48**, 2899–2903.
- M. Cokoja, C. Bruckmeier, B. Rieger, W. A. Herrmann and F. E. Kühn, *Angew. Chem., Int. Ed.*, 2011, **50**, 8510–8537.
- H. R. Moon, D. W. Lim and M. P. Suh, *Chem. Soc. Rev.*, 2013, **42**, 1807–1824.
- Z.-J. Lin, J. Lü, M.-C. Hong and R. Cao, *Chem. Soc. Rev.*, 2014, **43**, 5867–5895.
- J.-R. Li, J.-M. Yu, W.-G. Lu, L.-B. Sun, J. Sculley, P. B. Balbuena and H.-C. Zhou, *Nat. Commun.*, 2013, **4**, 1538.
- J. A. Mason, M. Veenstra and J. R. Long, *Chem. Sci.*, 2014, **5**, 32–51.
- Y.-N. Gong, Y.-L. Huang, L. Jiang and T.-B. Lu, *Inorg. Chem.*, 2014, **53**, 9457–9459.
- W.-Y. Gao, H.-F. Wu, K.-Y. Leng, Y.-Y. Sun and S.-Q. Ma, *Angew. Chem., Int. Ed.*, 2016, **55**, 5472–5476.
- P. Hu, J. V. Morabito and C.-K. Tsung, *ACS Catal.*, 2014, **4**, 4409–4419.
- Z.-B. Chen, Y. Zhang, Q. Yuan, F.-L. Zhang, Y.-M. Zhu and J.-K. Shen, *J. Org. Chem.*, 2016, **81**, 1610–1616.
- Z. Jiang, X. Xu, Y. Ma, H. S. Cho, D. Ding, C. Wang, J. Wu, P. Oleynikov, M. Jia, J. Cheng, Y. Zhou, O. Terasaki, T. Peng, L. Zan and H. Deng, *Nature*, 2020, **586**, 549–554.
- S. Sun, B.-B. Wang, N. Gu, J.-T. Yu and J. Cheng, *Org. Lett.*, 2017, **19**, 1088–1091.
- Y.-Y. Pan, Y.-N. Wu, Z.-Z. Chen, W.-J. Hao, G.-G. Li, S.-J. Tu and B. Jiang, *J. Org. Chem.*, 2015, **80**, 5764–5770.
- C. E. Houlden, M. Hutchby, C. D. Bailey, J. G. Ford, S. N. G. Tyler, M. R. Gagn, G. C. Lloyd-Jones and K. I. Booker-Milburn, *Angew. Chem., Int. Ed.*, 2009, **48**, 1830–1833.
- Y.-L. Sun, X.-B. Wang, F.-N. Sun, Q.-Q. Chen, J. Cao, Z. Xu and L.-W. Xu, *Angew. Chem., Int. Ed.*, 2019, **58**, 6747–6751.
- W.-Z. Zhang, H.-L. Li, Y. Zeng, X.-Y. Tao and X.-B. Lu, *Chin. J. Chem.*, 2018, **36**, 112–118.
- Z.-Q. Xue, P.-P. Huang, T.-S. Li, P.-X. Qin, D. Xiao, M.-H. Liu, P.-L. Chen and Y.-J. Wu, *Nanoscale*, 2017, **9**, 781–791.
- B.-B. Wang, S. Wang, J.-T. Yu, Y. Jiang and J. Cheng, *Org. Lett.*, 2017, **19**, 4319–4322.
- G. Férey, C. Mellot-Draznieks, C. Serre, F. Millange, J. Dutour, S. Surblé and I. Margiolaki, *Science*, 2005, **309**, 2040–2042.
- J. Pons, J. García-Antón, X. Solans, M. Font-Bardia and J. Ros, *Acta Crystallogr.*, 2008, **64**, M621–U163.
- M. Bahadori, S. Tangestaninejad, M. Monghadam, V. Mikhani, A. Mecher, I. Mohammadpoor-Baltork and F. Zadehahmadi, *Microporous Mesoporous Mater.*, 2017, **253**, 102–111.